Leucine-rich repeats and calponin homology containing 4 (Lrch4) regulates the innate immune response

Received for publication, June 4, 2018, and in revised form, November 27, 2018 Published, Papers in Press, December 6, 2018, DOI 10.1074/jbc.RA118.004300

Jim J. Aloor[‡1], Kathleen M. Azzam[‡], John J. Guardiola[‡], Kymberly M. Gowdy[‡2], Jennifer H. Madenspacher[‡], Kristin A. Gabor[‡], Geoffrey A. Mueller[§], Wan-Chi Lin[‡], Julie M. Lowe[‡], Artiom Gruzdev[¶], Michael W. Henderson[‡], David W. Draper[‡], B. Alex Merrick[‖], and Michael B. Fessler[‡3]

From the [‡]Immunity, Inflammation and Disease Laboratory, [§]Genome Integrity & Structural Biology Laboratory, [¶]Reproductive & Developmental Biology Laboratory, and [‖]National Toxicology Program, NIEHS, National Institutes of Health, Research Triangle Park, North Carolina 27709

Edited by Luke O'Neill

Toll-like receptors (TLRs) are pathogen-recognition receptors that trigger the innate immune response. Recent reports have identified accessory proteins that provide essential support to TLR function through ligand delivery and receptor trafficking. Herein, we introduce leucine-rich repeats (LRRs) and calponin homology containing 4 (Lrch4) as a novel TLR accessory protein. Lrch4 is a membrane protein with nine LRRs in its predicted ectodomain. It is widely expressed across murine tissues and has two expression variants that are both regulated by lipopolysaccharide (LPS). Predictive modeling indicates that Lrch4 LRRs conform to the horseshoe-shaped structure typical of LRRs in pathogen-recognition receptors and that the best structural match in the protein database is to the variable lymphocyte receptor of the jawless vertebrate hagfish. Silencing Lrch4 attenuates cytokine induction by LPS and multiple other TLR ligands and dampens the *in vivo* innate immune response. Lrch4 promotes proper docking of LPS in lipid raft membrane microdomains. We provide evidence that this is through regulation of lipid rafts as Lrch4 silencing reduces cell surface gangliosides, a metric of raft abundance, as well as expression and surface display of CD14, a raft-resident LPS co-receptor. Taken together, we identify Lrch4 as a broad-spanning regulator of the innate immune response and a potential molecular target in inflammatory disease.

Toll-like receptors (TLRs)[4] are an evolutionarily conserved family of pattern recognition receptors that are thought to detect select pathogen- and damage-derived (*i.e.* host) molecules in part through leucine-rich repeat (LRR) motifs in the TLR ectodomain (1). Ligation of TLRs, whether on the plasma membrane (TLR1, -2, -4, -5, and -6) or within endosomes (TLR3, -7, -8, and -9), triggers a complex series of signaling events through adaptor proteins and kinases, culminating in the activation of NF-κB and interferon regulatory factors (IRFs), master transcription factors that orchestrate the innate immune response via inducing pro-inflammatory cytokines and type I interferons. TLRs are pivotal for host defense but can also mediate inflammatory and autoimmune diseases (2, 3); thus, an improved understanding of their molecular regulation is expected to enrich our insight into human disease pathogenesis and to reveal new therapeutic targets (4).

Recent literature has revealed a growing number of accessory proteins that play essential roles in supporting TLR function (5). Thus, MD-2 assists TLR4 in binding of lipopolysaccharide (LPS) (6), RP105 regulates TLR4 signaling in a cell type–dependent manner (7, 8), CD14 regulates ligand interactions for multiple TLRs (5), and TRIL is thought to mediate ligand delivery to TLR3 and TLR4 (9). However, additional regulators such as GRP94 and PRAT4A serve as chaperones for multiple TLRs via facilitating proper protein folding and maturation (10, 11), whereas Unc93b1 interacts with multiple nucleic acid–sensing TLRs to mediate their delivery to endosomes (12).

Here, we introduce leucine-rich repeats and calponin homology containing protein 4 (Lrch4) as a novel accessory protein that regulates signaling by multiple TLRs. Lrch4 is predicted to be a single-pass transmembrane protein with approximately nine LRRs and a calponin homology (CH) motif in its ectodomain. It is widely expressed across murine tissues and is regulated by LPS. Lrch4 silencing attenuates cytokine induction by a wide array of TLR ligands in murine and human cells and also reduces inflammatory responses to LPS *in vivo*. Lrch4 co-precipitates with biotin-LPS from treated macrophages, suggesting interaction with LPS. Consistent with this, Lrch4 silencing reduces cell surface binding of LPS and alters the pattern of LPS

This work was supported by Grant Z01 ES102005 from the Intramural Research Program of the NIEHS, National Institutes of Health. The authors declare that they have no conflicts of interest with the contents of this article. The content is solely the responsibility of the authors and does not necessarily represent the official views of the National Institutes of Health.

This article contains Table S1 and Figs. S1–S3.

[1] Present address: East Carolina Diabetes and Obesity Institute, Dept. of Physiology, East Carolina University, Greenville, NC 27834-4354.

[2] Present address: Dept. of Pharmacology and Toxicology, East Carolina University, Greenville, NC 27834-4354.

[3] To whom correspondence should be addressed: NIEHS, National Institutes of Health, 111 T. W. Alexander Dr., P.O. Box 12233, MD D2-01, Research Triangle Park, NC 27709. Tel.: 919-541-3701; Fax: 919-541-4133; E-mail: fesslerm@niehs.nih.gov.

[4] The abbreviations used are: TLR, Toll-like receptor; LPS, lipopolysaccharide; Lrch4, leucine-rich repeat and calponin homology containing protein 4; LRR, leucine-rich repeat; MyD88, myeloid differentiation primary response 88; TMD, transmembrane domain; TRIF, Toll/interleukin-1 receptor domain–containing adapter-inducing interferon-β; IRF, interferon regulatory factor; CH, calponin homology; AA, amino acid(s); DAPI, 4′,6′-diamino-2-phenylindole; G-CSF, granulocyte–colony-stimulating factor; IL, interleukin; HDAC, histone deacetylase; TNF, tumor necrosis factor; qRT-PCR, quantitative RT-PCR.

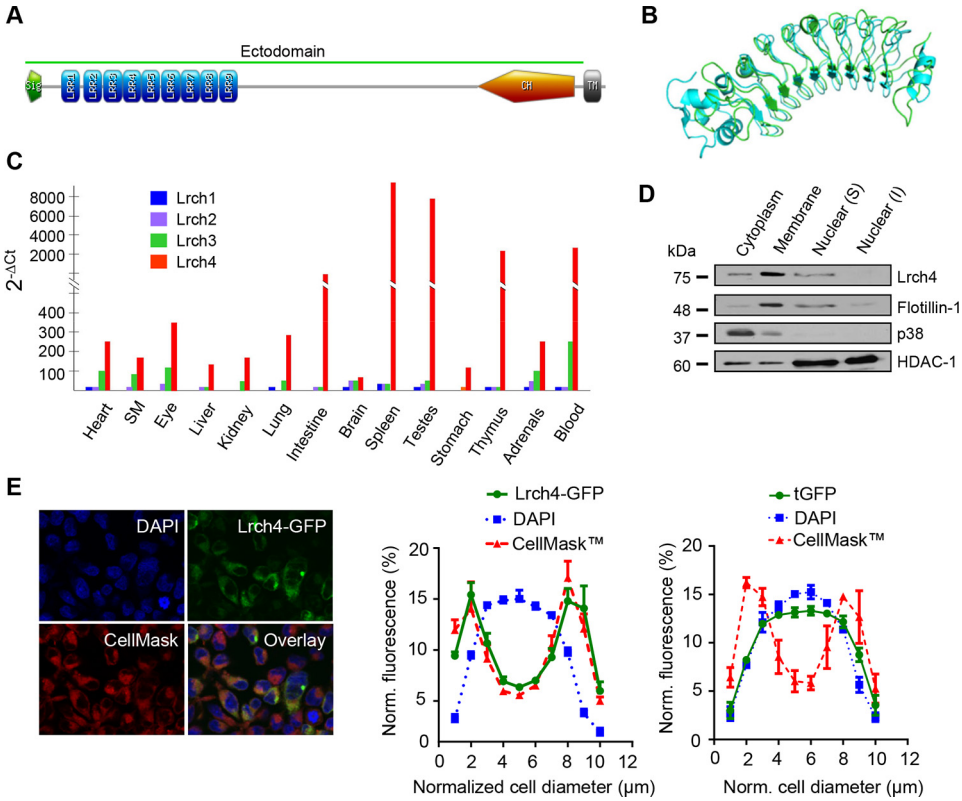

Figure 1. Basic structural and expression features of Lrch4. *A*, linear domain diagram of Lrch4 protein, generated using MyDomains Image Creator (https://prosite.expasy.org/; please note that the JBC is not responsible for the long-term archiving and maintenance of this site or any other third party hosted site). Lrch4 has a predicted ectodomain with an N-terminal 19-amino acid signal peptide (*Sig*) followed by nine LRRs, a calponin homology (*CH*) domain, a transmembrane domain (*TM*), and a short cytoplasmic tail. *B*, ribbon diagram model of the LRR domain of Lrch4 from BioSerf (*green*) compared with the best match in the Protein Data Bank (4PSJ, a synthetic construct of hagfish variable lymphocyte receptor; *cyan*) according to pGenThreader. *C*, expression of Lrch1, 2, 3, and 4 was profiled by qRT-PCR across 14 murine (C57BL/6J) tissues. *D*, the subcellular distribution of native Lrch4 within RAW 264.7 macrophages was biochemically profiled by immunoblotting of the fractions shown. Flotillin-1 serves as a membrane marker, p38 serves as a cytoplasmic marker, and HDAC serves as a nuclear marker. *S*, soluble; *I*, insoluble. *E*, the subcellular distribution of GFP-Lrch4 in TLR4-MD2-CD14-HEK293 cells was examined by confocal microscopy (40× objective, oil immersion; additional 50% zoom) in relation to the nuclear stain DAPI and the plasma membrane stain CellMask™ (*left*). Overlay of the three signals is shown in cellular cross-section using Zeiss Zen software (*middle*). By contrast, stably expressed tGFP vector control shows substantial overlay with DAPI (*right*). Images are representative of two independent experiments, both involving >10 high-power fields.

deposition on the macrophage, reducing LPS localization to rafts. Taken together, we identify Lrch4 as a broad-spanning regulator of the innate immune response with potential as a therapeutic target in inflammatory disease.

Results

Sequence, structural, and expression characterization of Lrch4

We recently identified Lrch4 in a proteomic screen as a protein increased in lipid raft microdomains of macrophages upon LPS exposure, suggestive of a potential role in TLR4 signaling (13). *Lrch4* (Gene ID: 231798) resides on chromosome 5 in the murine genome (7q22 in the human genome) and is predicted to have a 3,078-bp ORF (18 exons) that encodes a 680-amino acid (AA) protein (~73 kDa) with an pI of ~7.5. Sequence alignment using CLUSTAL (14) indicates a high degree of homology between murine *Lrch4* and human *LRCH4* (85.7%) and moderate homology between the human and zebrafish homologues (Fig. S1), suggesting significant evolutionary conservation. AA sequence-based prediction of conserved motifs (UniProt) in conjunction with transmembrane prediction (TMpred (15) and Philius (16)) indicates that Lrch4 has an ectodomain composed of a 19 AA N-terminal signal peptide followed by nine LRRs (each 21–23 AA in length), a central disordered region, and a CH motif; this is then followed by a transmembrane domain (TMD) and a short cytoplasmic tail (Fig. 1*A*).

Recent revisions of the NCBI and ENSEMBL database suggest that *Lrch4* has splice variants. The transcript support level is a method used by ENSEMBL to rate well-supported *versus* poorly supported transcript models. Three Lrch4 transcripts are identified at transcript support level 1 (*i.e.* all splice junctions of the transcript are supported by at least one nonsuspect mRNA). However, one of these (Lrch4-004) has incomplete 5′ and 3′ coding DNA sequences. We therefore focused on Lrch4-001 (referred to herein as variant 1) and Lrch4-002 (referred to as variant 2). Lrch4 variant 1 (680 AAs) is as described above, whereas variant 2 (649 AAs) is truncated C-terminal to the CH and omits the TMD, consistent with a soluble protein. Physiological expression of the predicted variants has not been verified to our knowledge.

LRRs are 20–30-AA motifs that exist in thousands of proteins across phylogeny, typically appearing as tandem repeats that together form a solenoid-shaped domain thought to mediate protein–ligand and protein– binding (17). Individual LRRs have been grouped based on sequence into seven categorical types, although the functional correlates of these categories remain unclear (18). Alignment of LRR domains between

murine *Lrch4* and human *LRCH4* suggests a very high degree of homology (Table S1), with manual inspection indicating that the majority of murine Lrch4 LRRs fall into the "plant-specific" LRR category, as was recently reported for human Lrch4 in a genome-wide survey of LRR proteins (18). Using the threading algorithm pDomTHREADER (19), the best structural match in the protein database to the LRR domain of Lrch4 is a protein derived from the variable lymphocyte receptor of the jawless vertebrate, the hagfish. The LRR region matches well to known LRR structures, whereas there is less confidence that the N and C termini are modeled accurately. As shown in Fig. 1*B*, predictive modeling of Lrch4 (*green*) based on the hagfish protein (*cyan*) yields the horseshoe-shaped structure typical of LRRs.

CH domains play a role in actin binding, although they may mediate additional interactions, especially when found singly rather than in tandem (20). A recent phylogenetic analysis indicated that the convergence of LRRs and CH domains in proteins (*i.e.* LRCH proteins) occurs rarely and only in animals, with just one protein (LRCH) in *Drosophila melanogaster* and four (Lrch1–4) in both *Mus musculus* and *Homo sapiens* (21). Interestingly, despite the very high degree of homology between murine *Lrch4* and human *LRCH4*, sequence alignment reveals modest homology between murine *Lrch4 and Lrch1* (35%), *Lrch4 and Lrch2* (34%), and *Lrch4 and Lrch3* (43%) (data not shown), suggesting divergent function among Lrch proteins.

Expression profiling of transcripts for the four *Lrch* family members indicates that Lrch4 (detected using primers common to the two variants) is widely expressed across 14 murine tissues, with the most abundant expression in spleen, testes, thymus, intestine, and blood (Fig. 1*C*). As shown in Fig. 1*D*, immunoblotting of murine macrophage subcellular fractions for endogenous Lrch4 (using an antibody targeting a region common to variants 1 and 2) confirms that it is predominantly present in the membrane, with lesser expression in the cytoplasm and soluble nuclear fraction, and is detected as a single band in all fractions. Consistent results showing a single band in both RAW 264.7 and primary murine macrophage lysates were obtained with both a commercial anti-Lrch4 antibody and an anti-Lrch4 antibody raised by our laboratory. Given that only variant 1 has a predicted TMD, this finding suggests that, at the protein level, variant 1 is expressed much more highly than variant 2 within the cell. Microscopy of GFP-Lrch4 in HEK293 cells reveals staining that includes a cytoplasmic-type pattern, but formal analysis indicates a high degree of overlap with the plasma membrane stain CellMask™ (Life Technologies) (22), in particular in cells with low-medium forced expression, consistent with substantial localization to the plasma membrane (Fig. 1*E*). By contrast, the tGFP vector (control) displays a very different distribution, largely overlapping the nuclear DAPI stain (Fig. 1*E*).

Lrch4 regulates cytokine induction by multiple TLRs

Based on its increase in rafts in response to LPS (13), its predicted receptor-like features, and its LRRs—a ligand-binding motif common to the ectodomain of all TLRs, as well as some TLR accessory proteins (CD14, RP105) (18)—we hypothesized that Lrch4 regulates TLR4 activation by LPS. To address this, we generated two stable Lrch4 lentiviral shRNA knockdown RAW 264.7 macrophage lines in parallel with a scrambled (Scr) lentiviral shRNA control line. As shown in Fig. 2*A*, compared with the Scr line, both knockdown lines achieved ≥50% silencing of Lrch4 mRNA (using probes common to both variants) and protein. Although this degree of knockdown is somewhat modest, it is consistent with past reports using RNAi in macrophages and likely reflects the relatively refractory nature of macrophages to transfection/transduction (23). Using variant-specific primers, we confirmed that both Lrch4 variants are expressed in the macrophage and that both are knocked down by Lrch4 shRNA (Fig. 2*B*). Of interest, LPS itself induced down-regulation of mRNA for Lrch4 variants 1 and 2 (Fig. 2, *A* and *B*).

Confirming a role for Lrch4 in regulation of TLR4 signaling, both Lrch4 knockdown lines induced significantly less TNFα than the Scr line in response to two doses of LPS (Fig. 2*C*). A similar reduction in LPS-induced TNFα was observed in two Lrch4 disruption clones produced by CRISPR-Cas9 (Fig. 2*D*). Given that some accessory proteins are reported to regulate signaling by multiple TLRs (*e.g.* CD14, TRIL (5)), we next tested a role for Lrch4 in additional TLR cascades. Lrch4 knockdown attenuated TNFα induction by the TLR1/2 ligand Pam3CSK4 (Fig. 2*E*), as well as by Pam2CSK4 (TLR2/6), imiquimod (TLR7), and ODN2395 (TLR9) (Fig. S2), indicating a broad-spanning role for Lrch4 in regulating plasmalemmal and endosomal TLRs. Induction of granulocyte–colony-stimulating factor (G-CSF) by both LPS and Pam3CSK4 was also reduced in Lrch4 knockdown cells, indicating that Lrch4 regulates multiple cytokines downstream of TLR2 and TLR4 (Fig. 2*E*). To test Lrch4 in human cells, we next silenced endogenous Lrch4 in HEK293 cells using an siRNA approach (Fig. 2*F*). HEK293 cells stably expressing either TLR4/MD-2/CD14 or TLR2 were transfected with Lrch4 siRNA or Scr siRNA and then exposed to LPS or Pam3CSK4, respectively. In preliminary experiments, we found that, in response to these stimuli, these cells produced very little TNFα (data not shown); thus, we surveyed for IL-8 protein production instead, as reported by others (24). As shown in Fig. 2*G*, Lrch4 siRNA attenuated IL-8 induction by both ligands in HEK293 cells, providing further support that the shRNA results in macrophages are unlikely to reflect off-target effects. Confirming some selectivity for Lrch4 function, Lrch4 silencing did not affect induction of IL-8 by HEK293 cells in response to stimulation with TNFα (Fig. 2*H*).

Lrch4 regulates both MyD88-dependent and MyD88-independent TLR4 signaling

We next focused on Lrch4 function in the TLR4 pathway. Moving further "upstream" of cytokine protein expression, we confirmed that Lrch4 knockdown also attenuates transcript expression of TNFα and G-CSF in response to LPS (Fig. 3, *A* and *B*). This suggested that Lrch4 may regulate LPS induction of pro-inflammatory cytokines at or upstream of transcription. The TLR4 cascade bifurcates immediately downstream of the receptor into two signaling arms defined by alternate usage of the cytoplasmic adaptors, myeloid differentiation primary response 88 (MyD88), and Toll/interleukin-1 receptor domain–containing adapter-induc-

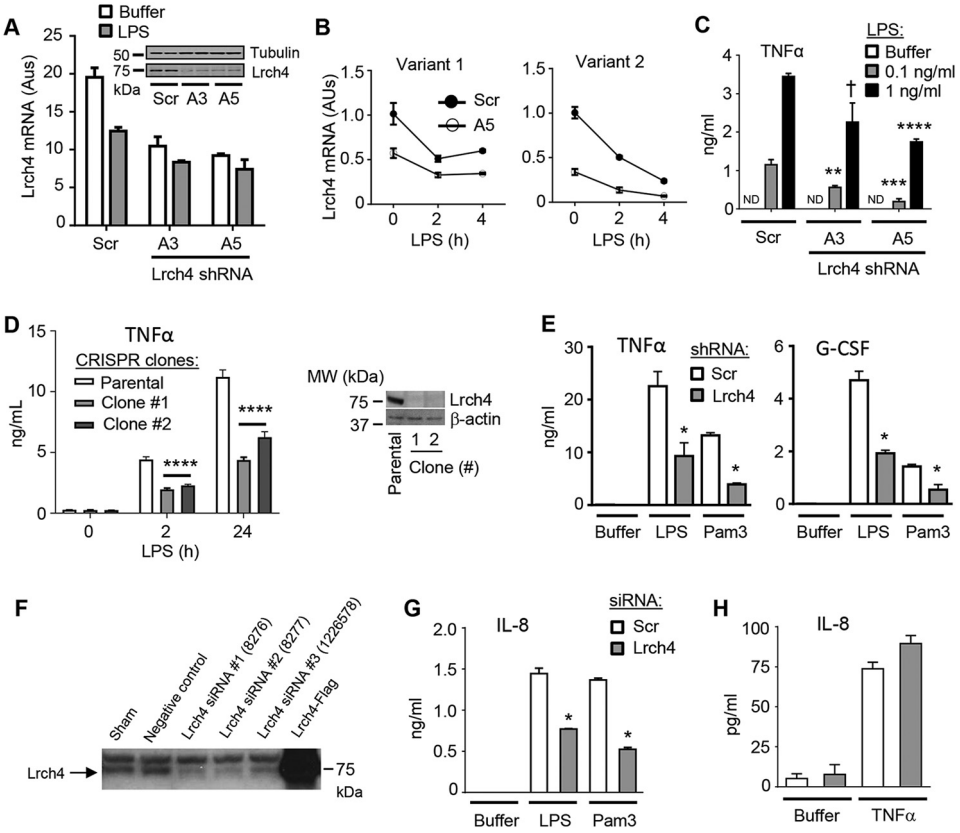

Figure 2. Silencing of Lrch4 attenuates macrophage responses to TLR ligands. *A*, silencing efficiency in RAW 264.7 macrophages of two stably transduced lentiviral Lrch4 shRNAs (A3 and A5) was evaluated at the transcript (graph; normalized to GAPDH as arbitrary units) and protein (immunoblot; samples in duplicate) level compared with a scrambled (Scr) control lentiviral shRNA. *B*, mRNA expression of Lrch4 variants 1 and 2 (normalized to 18S rRNA) was determined in Scr- and A5-transduced RAW 264.7 macrophages exposed to a time course of 10 ng/ml LPS. *C*, RAW 264.7 macrophages with Lrch4 (A3 and A5) or Scr lentiviral shRNA knockdown were exposed to buffer or two concentrations of LPS and then assayed by ELISA for TNFα protein release 2 h later. *ND*, not detected. *D*, two Lrch4 disruption clones were produced in RAW 264.7 cells by CRISPR-Cas9 and confirmed by Lrch4 immunoblot (*right*). The graph on the *left* shows TNFα protein release by the clones and parental controls in response to LPS (significant difference for both clones compared with parental at 2 and 24 h post-LPS). *E*, RAW 264.7 macrophages with Lrch4 (A5) or Scr knockdown were exposed to LPS (1 ng/ml) or Pam3CSK4 (10 ng/ml) and then assayed 2 h later by ELISA for TNFα or G-CSF release. *F*, HEK293 cells were sham-transfected (reagent only) or transfected with negative control siRNA, three alternate Lrch4 siRNAs, or FLAG-Lrch4 plasmid. Equal protein loads of whole cell lysate were then immunoblotted with anti-Lrch4 antibody as shown. *G*, HEK293-CD14-MD2 cells stably transfected with TLR4 or TLR2 were transfected with Scr/Lrch4 siRNA and then exposed to LPS (25 ng/ml) in the former case and Pam3CSK4 (100 ng/ml) in the latter case. IL-8 production was quantified by ELISA 8 h later. *H*, HEK293-CD14-MD2 cells were transfected with Scr or Lrch4 siRNA, exposed to buffer or TNFα (5 ng/ml), and then assessed by ELISA for IL-8 release 6 h later. All data are means ± S.E. and derive from at least three independent experiments. †, $p = 0.057$; *, $p < 0.05$; **, $p < 0.01$; ***, $p < 0.001$; ****, $p < 0.0001$.

ing interferon-β (TRIF) (1). These so-called "MyD88-dependent" and "MyD88-independent" pathways lead to downstream induction of distinct cytokines, although it is thought that most cytokines likely have some input from both adaptor pathways (25). Expression profiling of MyD88-dependent (Fig. 3*C*) and -independent (Fig. 3*D*) cytokines in LPS-stimulated macrophages after Lrch4 silencing indicated a role for Lrch4 in output from both adaptor arms, consistent with it regulating the proximal TLR4 pathway. However, differences in Lrch4 dependence were noted across cytokines, with some cytokines from both adaptor pathways showing dramatic reduction in Lrch4-silenced cells (*e.g.* IL-10, MCP-1), whereas other cytokines showed a more modest dependence on Lrch4 (*e.g.* IL-1β, IP-10). Taken together, these findings suggest that Lrch4 acts upstream of the MyD88/TRIF bifurcation in the TLR4 cascade.

Lrch4 regulates early signaling in the TLR4 cascade

Moving further upstream in the TLR4 cascade to confirm more directly whether Lrch4 regulates early signaling responses to LPS, we next evaluated activation of the transcription factors NF-κB and IRF3. NF-κB is activated by both an early MyD88-dependent and late MyD88-independent (TRIF-dependent) pathway after LPS, whereas IRF3 activation is generally thought to be dependent upon the TRIF pathway (26). As shown in Fig. 4*A*, activation of NF-κB in macrophage nuclear isolates was attenuated in Lrch4-silenced cells at both 15 and 30 min after LPS. LPS-induced NF-κB luciferase was also reduced in Lrch4-silenced RAW 264.7 macrophages (Fig. 4*B*). Finally, PO_4-IRF3 was also reduced in the nuclear fraction of Lrch4-silenced macrophages (Fig. 4*C*), indicating that Lrch4 is required for full LPS-induced activation of IRF3. Similar results for nuclear NF-κB activation, NF-κB luciferase, and PO_4-IRF3 were obtained using cells with CRISPR-Cas9–mediated disruption of Lrch4 (Fig. 4, *D–F*).

In addition to NF-κB and IRF3, LPS is well-known to lead to the rapid activation of MAPKs that, in turn, regulate multiple downstream functions including gene expression. Activation of these kinases is thought to be regulated by both MyD88 and

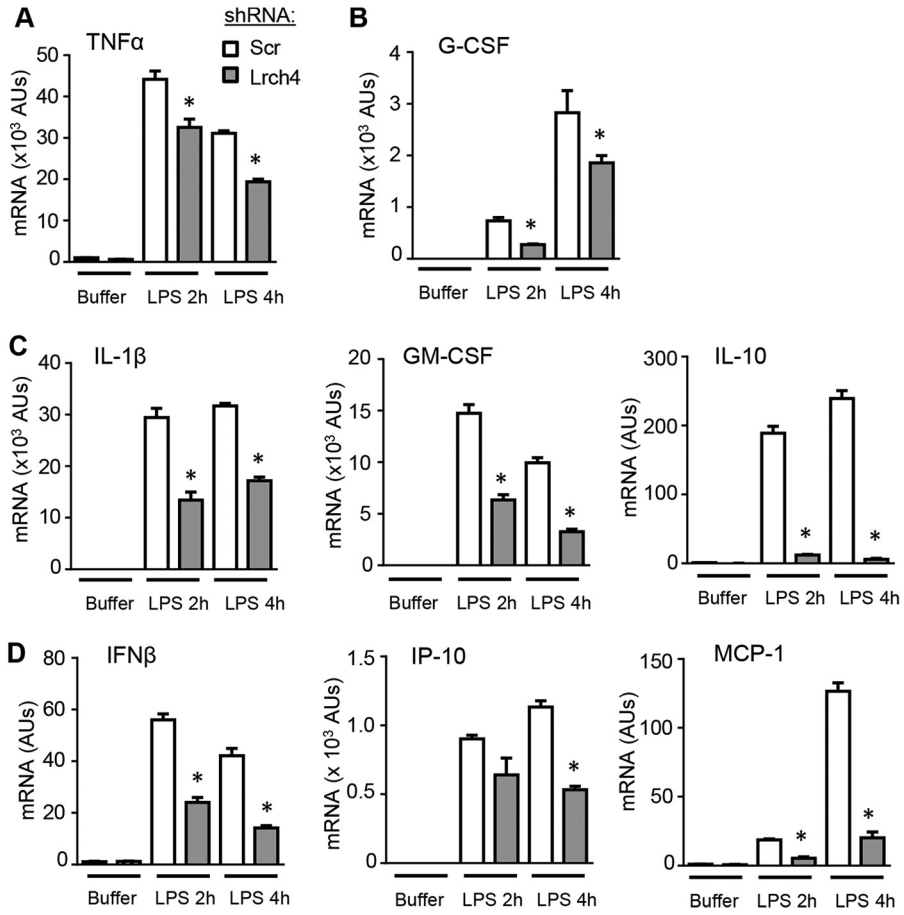

Figure 3. Lrch4 silencing attenuates pro-inflammatory cytokine expression. RAW 264.7 macrophages stably transduced with Lrch4 lentiviral shRNA (A5) or Scr control lentiviral shRNA were exposed to buffer or to LPS (10 ng/ml) for 2 or 4 h. Transcript abundance (normalized to GAPDH) was then quantified by qRT-PCR for TNFα (*A*), G-CSF (*B*), MyD88-dependent cytokines (*C*), and MyD88-independent cytokines (*D*) as shown. All data are means ± S.E. and derive from at least three independent experiments. *, $p < 0.05$. *AU*, arbitrary unit.

TRIF (26). As shown in Fig. 4*G*, Lrch4-silenced macrophages displayed a marked reduction in LPS-induced p38 activation (phosphorylation). By contrast, JNK phosphorylation was reduced at 15 min but not at 30 min post-LPS, consistent with a delay in its activation by LPS in Lrch4-silenced cells. Taken together, these results indicate that Lrch4 regulates early signaling events in the proximal TLR4 pathway, with effects upon both MyD88 and TRIF arms, but with varying temporal effects on the MAPKs.

Lrch4 regulates receptor-level events in the TLR4 pathway

Consistent with Lrch4 not exerting a global or indiscriminate effect upon TLR4 pathway output, we confirmed that neither silencing nor overexpression of Lrch4 altered cell surface display of TLR4 as assessed by flow cytometry (Fig. 5*A* and Fig. S3, *A* and *B*); nor did Lrch4 silencing or overexpression modify TLR4 gene expression (Fig. 5*B*). Similarly, Lrch4 knockdown had no effect on expression of the IL-6 receptor (Fig. S3*C*). Aiming to test whether Lrch4 could nonetheless impact ligand capture in the TLR4 pathway, we assessed cell-surface binding of LPS. Lrch4-silenced cells exhibited a significant, albeit modest reduction in overall surface binding of LPS (Fig. 5*C*). More remarkably, Lrch4-silenced cells showed reduced co-localization of LPS with the specific lipid raft marker cholera toxin subunit B (CtB; a ligand for the raft ganglioside GM1) (Fig. 5, *D* and *E*) (27, 28), in conjunction with a much more punctate surface deposition of LPS as quantified by number of LPS foci per cell (Fig. 5*F*). Together, this suggests that Lrch4 is not just required for quantitative surface capture of LPS, but more specifically for successful delivery of LPS to lipid rafts, the site where CD14 and the TLR4 receptor cluster and are thought to interact (29).

Testing more directly for a role of Lrch4 in LPS binding, we next performed a streptavidin bead pulldown after exposure of macrophages to biotin-LPS. As shown in Fig. 5*G*, Lrch4 was detected in the biotin-LPS pulldown (but not in cells treated with nonbiotinylated LPS, as expected), suggesting that it interacts either directly or indirectly with LPS. Lrch4 capture by biotin-LPS was effectively competed by nonbiotinylated LPS, consistent with a *bona fide* LPS interaction, whereas CD14 pulldown was not notably competed. This finding suggests either differing stoichiometry or avidity to LPS of the two proteins.

We also tested for an effect of Lrch4 on CD14 given that CD14 plays a critical role in delivery of LPS from LPS-binding protein to TLR4/MD2 in lipid rafts (as well as in receptor-level interactions in the TLR2 and TLR7 cascades (5)). Lrch4-silenced macrophages had a significant reduction in cell surface

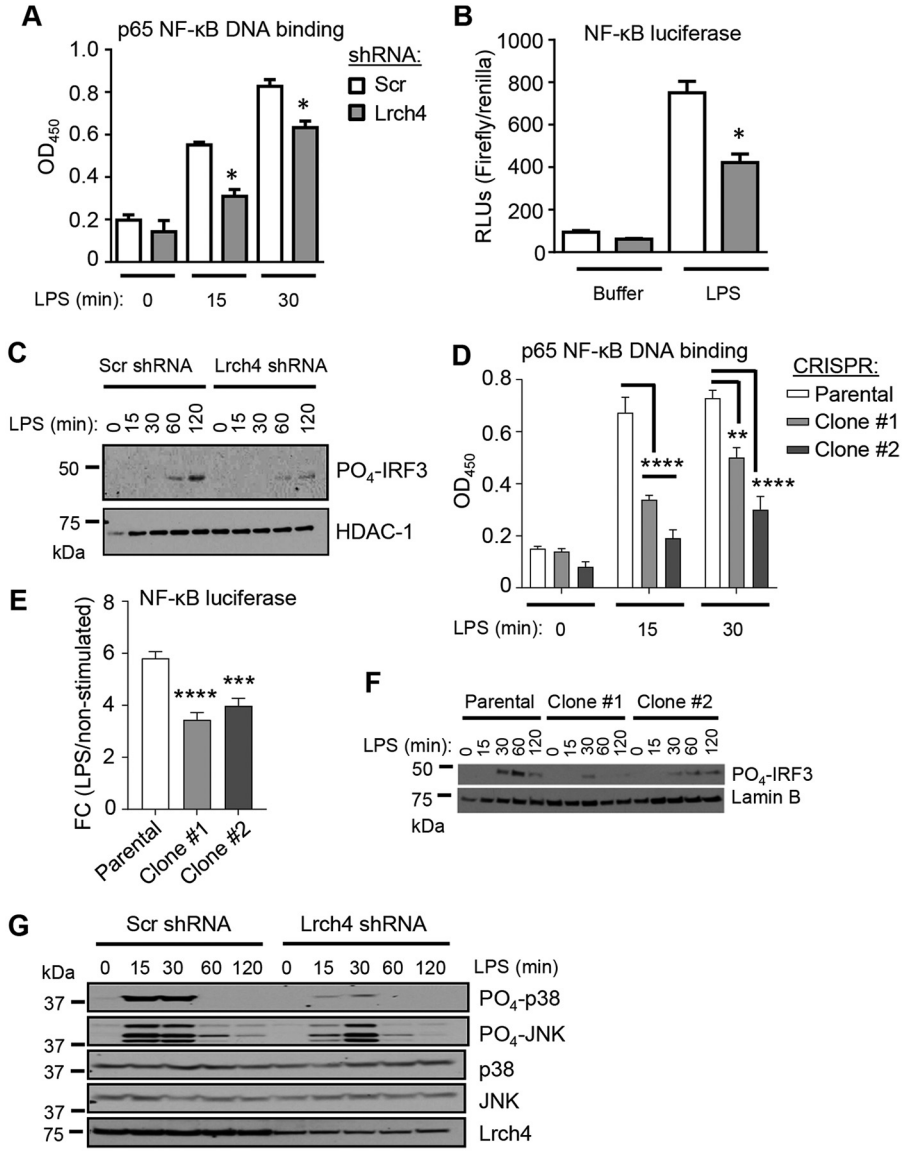

Figure 4. Lrch4 silencing attenuates activation of pro-inflammatory transcription factors and kinases. *A*, RAW 264.7 macrophages stably transduced with Lrch4 lentiviral shRNA (A5) or Scr control lentiviral shRNA were exposed to buffer or to LPS (1 ng/ml) for 15 or 30 min. Activated p65 NF-κB was then quantified in equal protein aliquots of nuclear isolates. *B*, cells as in *A* were transfected with NF-κB–driven firefly luciferase and *Renilla* luciferase plasmids and exposed to buffer or to LPS (10 ng/ml) for 8 h. Relative luciferase units (*RLUs*) were then quantified by luminometry in cell lysates. *C*, cells as in *A* were exposed to LPS as shown. Nuclear isolates were then probed for PO_4-IRF3 and HDAC-1 (loading control). *D–F*, two Lrch4 CRISPR-Cas9 clones and parental RAW 264.7 cells were stimulated and assayed as in *A–C*. In *E*, fold change (*FC*) in firefly/*Renilla* RLUs in the LPS-stimulated state compared with the nonstimulated state is shown. *G*, RAW 264.7 macrophages stably transduced with Lrch4 lentiviral shRNA (A5) or Scr control lentiviral shRNA were exposed to LPS (1 ng/ml) as shown. Equal protein aliquots of whole cell lysate were then probed by immunoblot for the indicated targets. The data in *A*, *B*, *D*, and *E* are means ± S.E. The data derive from at least three independent experiments. *, $p < 0.05$; **, $p < 0.01$; ***, $p < 0.001$; ****, $p < 0.0001$

display, protein expression, and transcript expression of CD14 (Fig. 5, *H–J*, and Fig. S3*D*). This may suggest that Lrch4 promotes LPS capture, raft delivery, and signaling at least in part through a mechanism involving up-regulation of CD14. However, our experiments in HEK293 cells involved plasmid-based stable overexpression of CD14, which we confirmed was not reduced by Lrch4 silencing (Fig. S3*E*). Lrch4 regulation of LPS signaling is thus unlikely to derive solely from CD14 regulation. Several TLRs are thought to be activated in lipid raft microdomains and to require raft abundance and integrity for intact signaling (30). Cells with chemically disrupted rafts have defective responses to LPS (29). Suggesting that Lrch4 may be required for lipid raft maintenance, we found that Lrch4-silenced macrophages had significantly reduced raft signal, as assessed by CtB staining (Fig. 5, *D* and *K*) (27, 28).

Lrch4 regulates the innate immune response in vivo

The innate immune response plays a central role in a wide range of human diseases (4). Our studies in macrophage culture thus prompted us to examine a potential role for Lrch4 in the innate immune response *in vivo*. To test a potential role for Lrch4 in the response to LPS in the lung, we locally silenced Lrch4 in the airway of C57BL/6 mice by intratracheal delivery of lentiviral shRNA using published techniques (31, 32). Lrch4 immunoblotting of whole lung homogenates confirmed a ~50% knockdown of Lrch4 with either of two lentiviral con-

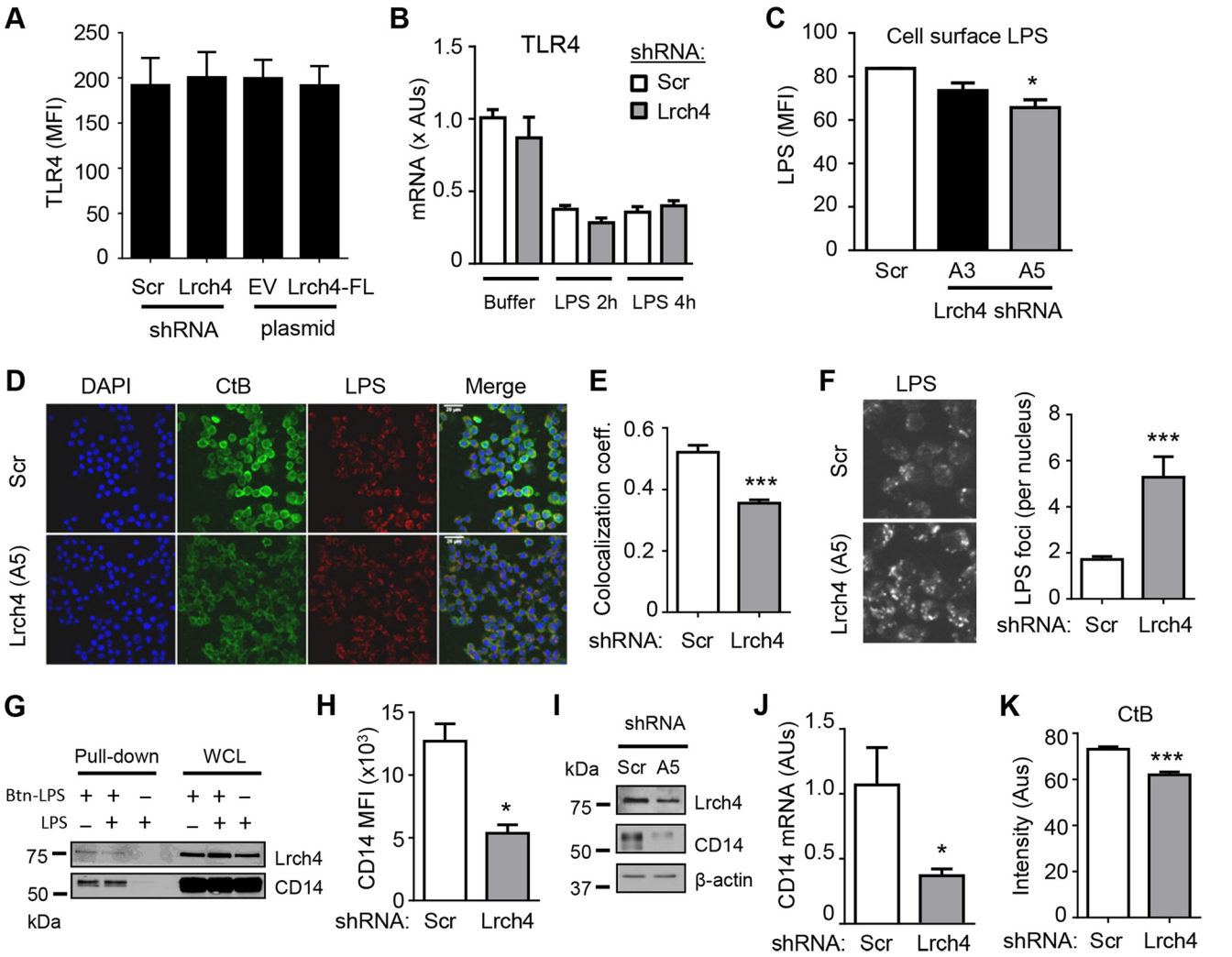

Figure 5. Lrch4 regulates receptor-level interactions in LPS pathway. *A*, cell surface display of TLR4 was quantified in RAW 264.7 macrophages stably transduced with Lrch4 (A5) or Scr control lentiviral shRNA and in RAW 264.7 macrophages transfected with Lrch4-FLAG or empty vector (*EV*) plasmids. *B*, cells stably transduced with lentiviral shRNAs as in *A* were exposed to buffer or LPS as shown, after which normalized TLR4 mRNA was quantified by qRT-PCR. *C*, cells stably transduced with Scr or Lrch4 (A3 and A5) lentiviral shRNAs were exposed to biotin-LPS and then to AF633-streptavidin and evaluated by flow cytometry. *D*, Scr and Lrch4 shRNA macrophages were treated with CtB-AF488 and LPS-biotin/APC-streptavidin, co-stained with the nuclear stain DAPI, and then imaged (63× objective; oil immersion). *E*, co-localization of LPS and CtB signals was quantified using Zeiss Zen software for cells processed in *D*. *F*, LPS deposits as in *D* are shown without pseudocoloring to aid in visualization and with a further 5× magnification in ImageJ software (*left*). Discrete foci of LPS signal were quantified for cells in *D* using MetaMorph (*right*). *G*, RAW 264.7 macrophages were treated with biotin-LPS and/or LPS. Whole cell lysate (*WCL*) and streptavidin-agarose pulldowns from cell lysates were then immunoblotted for Lrch4 and CD14. *H–J*, CD14 was quantified by flow cytometry (*H*), immunoblot of cell lysate (*I*), and qRT-PCR (*J*) in RAW 264.7 macrophages stably transduced with Scr or Lrch4 (A5) lentiviral shRNA. *K*, Scr and Lrch4 shRNA cells were processed as for microscopy in *D*. CtB staining was quantified using MetaMorph software. The data are means ± S.E. and derive from at least three independent experiments. *, $p < 0.05$; **, $p < 0.01$; ***, $p < 0.0001$. *MFI*, mean fluorescence intensity; *AU*, arbitrary unit.

structs compared with Scr control (Fig. 6, *A* and *B*). The mice were then challenged with aerosolized LPS (33). As shown in Fig. 6 (*C* and *D*), compared with Scr control, Lrch4 silencing did not alter steady state cell counts in the airway of unexposed mice. However, Lrch4 silencing by either of two alternate lentiviral constructs was associated with a marked reduction in influx of leukocytes into the airway after LPS, largely reflecting a reduction in neutrophils. This finding suggests that Lrch4 plays a modulatory role in the innate immune response *in vivo*.

Discussion

TLRs play a key role in a wide range of inflammatory diseases in addition to detecting pathogens and inducing host defense responses. In recent years, a growing list of proteins have been identified that support signaling by TLRs, some of these acting as accessory proteins for several TLRs (5). TLR accessory proteins act through a wide range of mechanisms, including ligand delivery/binding, TLR folding/processing, and TLR trafficking. Here, we introduce Lrch4, a ~73-kDa transmembrane LRR-containing protein that supports signaling by both plasmalemmal TLRs (TLR1/2, TLR2/6, and TLR4) and endosomal TLRs (TLR7 and TLR9).

In the TLR4 pathway, Lrch4 promotes early events, including both MyD88-dependent and MyD88-independent signaling. We provide evidence that this may stem from its role in promoting LPS binding, and, in particular, delivery of LPS to lipid rafts, the membrane microdomain where LPS and other microbial ligands are transferred from carrier proteins such as LPS-

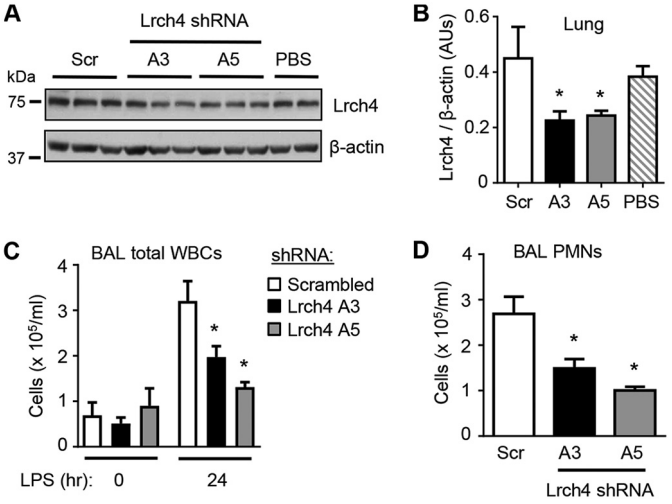

Figure 6. Lrch4 regulates the innate immune response *in vivo*. *A* and *B*, C57BL/6 mice were treated by oropharyngeal aspiration with 1× PBS (pH 7.4), or scrambled control (Scr) or Lrch4 (A3 and A5) lentiviral shRNAs. 5 days later, Lrch4 and β-actin (loading control) were quantified in equal protein aliquots of lung homogenate by immunoblot (*A*). Replicate lanes represent data from independent animals. Corresponding densitometry is shown in *B*. *AUs*, arbitrary units. *C* and *D*, mice treated as in *A* were left untreated or were exposed to aerosolized LPS (300 μg/ml, 30 min). Total leukocytes (*WBCs*) (*C*) and neutrophils (PMNs) (*D*) were quantified in bronchoalveolar lavage (*BAL*) 24 h later. The data are means ± S.E. and derive from at least three independent experiments involving $n = 5$ mice/treatment/time point. *, $p < 0.05$ for comparison to Scr.

binding protein to the common TLR co-receptor, CD14 (5, 29). CD14, a raft-resident protein previously shown to support signaling by TLRs -2, -3, -4, -7, and -9 via multirecognition ligand binding (5), is down-regulated in Lrch4-silenced cells, offering a potential unifying mechanism for Lrch4 action across TLRs. The role of Lrch4 in TLR4 signaling, however, appears to extend beyond CD14 as Lrch4 silencing attenuates LPS responses in cell lines with plasmid-based stable expression of CD14.

LRRs, 20–30-residue motifs typically found in tandem chains ranging from 2 to 45, occur in thousands of proteins throughout phylogeny and are thought to mediate protein–ligand and protein–protein interactions (17, 18). In addition to an established role in innate immunity, they are involved in a wide range of cellular processes, including apoptosis, neuronal development, autophagy, and nuclear mRNA transport. Of the ~375 LRR-containing proteins in humans, the majority have no known function (18). In *Drosophila*, the single *LRCH* gene has been recently shown to play a role in cytoskeletal remodeling during apoptosis (21), but limited homology (~32%) exists between *D. melanogaster LRCH* and *M. musculus Lrch4*. Although the four mammalian Lrch genes/proteins have never previously been investigated to our knowledge, a few recent genome-wide screens have made incidental findings relating to Lrch4. Thus, Lrch4 has been found to be among LRR proteins that are down-regulated in human macrophages in response to bacterial infection (18), to be present in the phagosomes of mycobacterial-infected macrophages (34), to be among genes regulated by miR-155 in LPS-stimulated dendritic cells (35), and to increase with age in the human brain (36). Collectively, these reports have suggested a role for Lrch4 in host defense and perhaps in human disease.

We predict that, as has been the case for virtually all other TLR accessory proteins described to date, broader roles may ultimately be identified for Lrch4 in cell biology and immunity than defined in this report. As may be suggested by its apparent effect on rafts and CD14, Lrch4 may regulate cellular responses to a wider array of ligands, directly or indirectly, and perhaps function in more than one location/role within the cell. Our finding that Lrch4 silencing has differential effects across cytokine transcripts could suggest that it has regulatory effects on the TLR4 pathway from a location at or downstream of transcription factor activation. Alternatively, as we suggest, Lrch4 could exert selective effects from a receptor-proximal location, given that CD14 itself has been shown to have differential effects on MyD88-dependent and -independent signaling (37) and even to mediate TLR4-independent responses to LPS (38).

Our attempts to ectopically express and purify adequate quantities of soluble Lrch4 or portions of its ectodomain for *in vitro* studies of ligand binding were unsuccessful because of difficulties with protein insolubility/folding (not depicted). Our detection of a single band for endogenous Lrch4 in all subcellular fractions, soluble and membranous, suggests that the putative nontransmembrane variant of Lrch4, if expressed as protein, may either be expressed at very low levels or, alternatively, be secreted from the cell, analogous to soluble CD14, MD-2, and TLRs (5, 39). Future studies will be required to determine whether Lrch4 binds LPS directly and whether soluble Lrch4 facilitates detection or acts as a decoy (with possible therapeutic implications) for microbial molecules. Finally, the predicted extracellular location of the CH motif in Lrch4 is of uncertain significance. Single CH motifs are thought to be insufficient to bind actin but are reported to mediate protein–protein interactions with a variety of other motifs and proteins, including signaling proteins (20).

A potential cross-cutting mechanism by which Lrch4 may regulate multiple TLRs is via assembly/organization of lipid rafts. Multiple TLRs are thought to be activated in raft-like membrane microdomains and to be sensitive to raft composition (30). We found that Lrch4 regulates the raft molecules GM1 and CD14, the latter at the level of transcript abundance. Intracellular mediators of CD14 transcription have been defined, including cAMP (40) and transcription factors, such as AP1, Sp1, C/EBP, and STAT1 (41–43), several of these regulating CD14 in response to extracellular signals. Similarly, although rafts are thought to be assembled through complex protein–lipid interactions that begin in the Golgi (30), raft abundance on the cell surface as assessed by CtB is also sensitive to extracellular signals. For example, high-density lipoprotein and apolipoprotein E reduce CtB signal and raft-dependent signaling (44, 45), whereas extracellular cholesterol increases both readouts (46, 47). We speculate that Lrch4 regulation of rafts and CD14 may operate through sensitizing the macrophage to external signals (*i.e.* serum factors).

Additional possible mechanisms of TLR regulation are consistent with our findings. Analogous to other raft proteins such as the flotillins (48), multimerization of Lrch4 itself or Lrch4-mediated protein–protein interactions within rafts may regulate raft topography. Alternatively, Lrch4 may serve as a raft chaperone for TLRs, regulating their successful trafficking to

microdomains where they complex with signaling partners. Future studies, perhaps using super-resolution microscopic techniques, will be required to resolve these possibilities and to more comprehensively characterize the role of Lrch4 in determining raft size and composition.

TLR signaling has been shown to contribute to a wide range of noninfectious inflammatory diseases, likely through detection of host-derived molecules that are increased during disease (*i.e.* "damage-associated molecular patterns" such as hyaluronic acid, oxidized LDL, and fatty acids (49)). This has elevated TLRs as targets of intense interest for drug development and has also suggested that TLR accessory proteins may represent cross-cutting therapeutic targets for a variety of diseases ranging from atherosclerosis to cancer to autoimmune disease (4). We speculate that Lrch4 may also regulate pro-inflammatory TLR signaling responses to host-derived molecules and may potentially represent a novel therapeutic target in human disease.

Experimental procedures

Reagents

Pam3CSK4, Pam2CSK4, imiquimod, and ODN2395 were from InvivoGen (San Diego, CA); *Escherichia coli* 0111:B4 LPS from List Biological (Campbell, CA); Dulbecco's modified Eagle's medium and fetal bovine serum from ATCC (Rockville, MD); and polymyxin B, *E. coli* 0111:B4 LPS (for *in vivo* studies), penicillin, and streptomycin from Sigma.

Cell culture

RAW 264.7 macrophage cells (ATCC, Manassas, VA; ATCC TIB-71) and HEK293-MD2-CD14 cells (Invivogen, San Diego, CA) were cultured in Dulbecco's modified Eagle's medium supplemented with 10% heat-inactivated fetal bovine serum, 100 μg/ml streptomycin, and 100 units/ml penicillin in a humidified 5% CO_2 atmosphere at 37 °C. Cells were exposed to stimuli as described.

Lrch4 silencing in RAW 264.7 macrophages

A lentiviral set of five shRNA against murine Lrch4 was purchased from Open Biosystems/Thermo Fisher. Lentiviral packaging was achieved by using Lipofectamine 2000 (Invitrogen) to transiently transfect HEK293T/17 cells (ATCC no. SD-2515) with the desired shRNA in a pLKO.1 vector together with vesicular stomatitis virus G glycoprotein and packaging plasmids according to standard protocols (50). Supernatant was collected 48 h post-transfection and concentrated by centrifugation (50,000 $\times$ *g*, 2 h). Pellets were resuspended in PBS and used for infection. All titers were determined by performing quantitative PCR to measure the number of lentiviral particles that integrated into the host genome. In addition to quantitative PCR, biological titration of viruses that co-expressed fluorescent moieties was determined by flow cytometry. RAW264.7 murine macrophage cells were infected with sh-lentivirus at a multiplicity of infection of 100 and at 48 h post-infection were selected with 10 μg/ml puromycin (Calbiochem) for ~9 days. Lrch4 silencing was assessed by immunoblotting. Two of the five shRNA were determined to be most effective; the target sequences of those shRNAs and the sequence for the negative control (scrambled shRNA) are: (i) A3 (TRCN0000121334), CCGGGCTCTCAAGTCTCGGAAGAATCTCGAGATTCTTCCGAGACTTGAGAGCTTTTTG; (ii) A5 (TRCN0000121336), CCGGCCTTCTGAATTAAGCCTTGTACTCGAGTACAAGGCTTAATTCAGAAGGTTTTTG; and (iii) Scrambled shRNA, CCTAAGGTTAAGTCGCCCTCGCTCGAGCGAGGGCGACTTAACCTTAGG.

Lrch4 deletion by CRISPR-Cas9

Lrch4-deficient RAW 264.7 cells were generated with CRISPR/Cas9-mediated excision of exon 2, which results in disruption of the LRR domain. Cas9 guides were designed to target the intronic sequence flanking exon 2; AAGGTTCGGCCTCACACAAT[NGG] and GTCTGGGAGAACCATTCGGG[NGG]. Complimentary guide oligonucleotides were cloned into the BbsI restriction site of pSpCas9(BB)-2A-GFP (PX458), a gift from Feng Zhang (51). Clones were screened for exon 2 excision/disruption with amplicon sequencing with primers flanking the Cas9 target sites and exon 2: forward, 5′-CTGTTGTTCAGGTACCATCCACT-3′; and reverse, 5′-CTGATGATAAGCACTCGAAGGGG-3′. WT locus amplicon was 709 bp, and the guide-to-guide exon 2 excised locus amplicon was 466 bp (actual size variable because of nonhomologous end-joining repair of Cas9-mediated double-stranded breaks).

Transfection of HEK293-MD2-CD14 cells

HEK293-hMD2-CD14 cells (Invivogen) were stably transfected with pUNO-hTLR2-HA (Invivogen) or hTLR4 (a gift from Ruslan Medzhitov; Addgene plasmid no. 13086) using standard antibiotic selection procedures. Lrch4-specific siRNA (Silencer(R) Select siRNA for human Lrch4, identification no. s8276; catalog no. 4392420) GTCTGGAAATGAGTCAACA or negative control siRNA (Silencer negative control 1 siRNA; catalog no. AM4611) were transfected using Lipofectamine 2000 (Invitrogen) per the manufacturer's instructions, in serum-free OptiMEM (Gibco–Invitrogen). Transfected cells (48 h post-transfection) were then used for experiments. In experiments requiring plasmid transfections, the cells were either co-transfected with the siRNA or sequentially transfected with siRNA followed by plasmids 24 h later.

NF-κB luciferase assay

FuGENE HD (Promega, Madison WI) transfection reagent was used (4.4 μl/μg DNA) to co-transfect RAW264.7 cells with reporter plasmid pNFκB-Luc (Clontech) and with pRL-TK (Promega) as transfection normalization control. 48 h post-transfection, the cells were washed, fresh media were added, and the samples were either left untreated or treated with a ligand for 8 h. The cells were washed and lysed with passive lysis buffer, and luciferase activity was assessed using dual luciferase assay (Promega) measured on a Biotek Synergy 2 plate reader.

Western blotting

The cells were lysed, and equivalent loads of total protein were separated by SDS-PAGE, transferred to nitrocellulose membranes, and blocked in 5% milk/TTBS. Membranes were probed with antibodies against phospho-p38 (Thr-180/Tyr-

182; Cell Signaling), phospho-JNK (Thr-183/Tyr-185; Cell Signaling), p38 (C-20: sc-535; Santa Cruz), JNK1 (C17:sc-474; Santa Cruz), IκBα (C-21; sc-371; Santa Cruz), Lrch4 (D20: sc-51421, Santa Cruz), flotillin-1 (BD Biosciences), histone deacetylase (HDAC)-1, PO_4-IRF3 (Cell Signaling Technology, Inc., Danvers, MA), and CD14 (BD Pharmingen, San Diego, CA). Signal was detected by species-specific HRP-conjugated secondary antibodies, followed by standard chemoluminescence and exposure to film.

p65 NF-κB activation assay

Nuclear extracts were isolated using the NE-PER kit (Pierce) per the manufacturer's instructions. Equal nuclear protein aliquots (Pierce BCA assay) were then analyzed with the TransAM NF-κB p65 kit (Active Motif) per the manufacturer's conditions.

Cytokine protein measurement

Media supernatants were analyzed by either the Bioplex multiplex bead assay (Bio-Rad) or ELISA to mouse TNFα or human IL-8 (BioLegend) per the manufacturer's specifications.

RNA isolation, reverse transcription, and quantitative PCR

RNA was isolated by RNEasy kit (Qiagen). cDNA were generated using TaqMan reverse transcription reagents from Applied Biosystems (Foster City, CA). Real-time PCR was performed in duplicate with TaqMan PCR mix (Applied Biosystems) in the HT7900 ABI sequence detection system (Applied Biosystems). Predesigned, validated TaqMan primer/probe sets for murine Lrch4 (Mm00461397_m1), GAPDH (Mm99999915_g1), Cxcl10/IP-10 (Mm00445235_m1), IFNβ (Mm00439552_s1), Csf2/GM-CSF (Mm01290062_m1), IL1β (Mm00434228_m1), TNFα (Mm00443258_m1), IL10 (Mm00439614_m1), IL6-Rα (Mm00439653_m1), and TLR4 (Mm00445273_m1) were purchased from Applied Biosystems. Gene expression was normalized to GAPDH and expression levels in untreated control samples were set as a value of 1.0. SYBR-green quantitative PCR methodology using an ABI Prism 7900HT was utilized to determine Lrch4 variant expression using the primers: Lrch4 V1 forward, GGAGGCTGTGATCCTGGTTG; Lrch4 V1 reverse, CCGAGTGTAGACGACATAGAG; Lrch4 V2 forward, GAAAATGGGTGTGCCTGAGGAG; and Lrch4 V2 reverse, ACCTCTACCCCTAAGGCTGTT.

Anti-Lrch4 antibody production

Keyhole limpet hemocyanin–conjugated peptide [H]-CSPAVPKLSALKSRKNVES-[NH_2] was synthesized and purified by Princeton Biomolecules (Langhorne, PA). Purified peptide was injected (with Freund's adjuvant) into rabbits by Harlan Laboratories (Indianapolis, IN) to generate custom polyclonal antibody to Lrch4 using routine procedures. Antibody specificity was validated by Lrch4 shRNA and CRISPR-Cas9 (see "Results").

Subcellular fractionation

Macrophages were resolved into membrane, cytosolic, and nuclear fractions using a subcellular protein fractionation kit (Thermo Scientific) per the manufacturer's instructions.

Murine in vivo exposures

C57BL/6J female mice, 8–10 weeks old and weighing 18–22 g, were used and were from the Jackson Laboratory. All experiments were performed in accordance with the Animal Welfare Act and the U.S. Public Health Service Policy on Humane Care and Use of Laboratory Animals after review and approval by the Animal Care and Use Committee of the NIEHS, National Institutes of Health. Lentiviral shRNA (scramble control or Lrch4 specific; 6×10^7 transduction units in 50 μl of saline) was delivered to the lung by oropharyngeal aspiration during isoflurane anesthesia, similar to past reports (31, 32). Exposure to aerosolized LPS (300 μg/ml, 30 min) was as previously described (33).

Bronchoalveolar lavage fluid collection and analysis

Bronchoalveolar lavage fluid was collected immediately following sacrifice and cell counts performed as described (33).

Flow cytometry analysis of CD14 and TLR4 surface expression

The cells were processed for flow cytometry as previously reported (33). Anti-mouse CD284 (TLR4) phycoerythrin (12–9041), anti-mouse CD14 phycoerythrin (12–0141), and isotype control antibodies were from eBioscience (San Diego, CA). Flow cytometry was performed using an LSR II (BD Biosciences) and analyzed using FlowJo software (Tree Star, Inc., Ashland, OR).

Structural prediction of Lrch4

The structure of the Lrch4 LRR domain was modeled based on bioinformatics analyses. The LRR region is predicted to extend to residue 249. However, predictions of disorder from residues 250 to 327 give reduced confidence, suggesting there may be some structure. After residue 327, the predictions of disorder become highly confident until the start of the CH domain near residue 535 (52). To ascertain whether residues 1–327 were structured, this sequence fragment was submitted to pGenTheader for comparison to known protein structures. The best matches only contain structured residues up the end of the LRR domain, except in a few cases where the sequence matches to a fragment of much longer LRR (>600 residues). We view these exceptions as unlikely because these are very large proteins with many LRRs that are clearly not present in Lrch4. Residues 250–327 were searched alone for structural matches, but none were found with statistical confidence. The region is likely unstructured. The structure of the LRR in Fig. 1 was modeled from Protein Data Bank code 4PSJ with Bioserf.

LPS binding

LPS binding was measured by incubating the RAW 264.7 macrophages (1×10^6) with 5 μg/ml of biotin-labeled LPS (Invivogen) at 37 °C for 15 min. Surface binding was assessed with streptavidin-APC (BD Biosciences). LPS signal was quantified by flow cytometry using an LSR II (BD Biosciences) and analyzed using FlowJo software (Tree Star, Inc.).

Confocal microscopy

TLR4-MD2-CD14-HEK293 cells were plated overnight on poly-L-lysine–coated coverslips or 8-well chamber slides (Nunc, Rochester, NY). The cells were either sham-transfected or trans-

fected with tGFP or hLrch4-tGFP. 48 h post-transfection, the cells were left unstained or stained with 1× CellMask™ Orange plasma membrane stain (Molecular Probes/Life Technologies) for 5 min at 37 °C, followed by fixation (4% formaldehyde). After three washes, the coverslips were mounted in ProLong Gold antifade reagent containing DAPI and imaged as described below. Scrambled or Lrch4 shRNA RAW264.7 cells were plated overnight on MatTek dishes (Ashland, MA) or 24-well plates. The cells were left untreated or treated with 100 ng/ml biotin-LPS for 10 min at 37 °C. The cells were then either left unstained or stained (10 min, 4 °C) with 1 μg/ml of cholera toxin subunit B-Alexa Fluor 488 conjugate (Molecular Probes/Life Technologies). The cells were then washed thrice, fixed, and blocked (2% BSA in PBS-T, supplemented with 20% fetal bovine serum) overnight. Some wells/dishes were additionally stained with Alexa Fluor 633-conjugated streptavidin. After three washes, the wells/dishes were mounted in ProLong Gold antifade reagent containing DAPI and imaged as described below. Imaging was performed using a Zeiss LSM 710 (Carl Zeiss). For CtB and LPS, objective conditions were Plan-Apochromat 63×; NA = 1.40; oil immersion. For Lrch4 and CellMask™, objective conditions were EC Plan-Neofluar 40×; NA = 1.3; oil immersion. Cholera toxin (CtB-AF488) intensity and LPS foci were analyzed using MetaMorph software, and Lrch4-LPS co-localization was analyzed using Zeiss Zen software.

Co-precipitation studies

Co-precipitation studies were undertaken to assess the ability of Lrch4 to associate with LPS in cells treated *in vivo*. RAW 264.7 macrophages were incubated (15 min, 37 °C) with either 10 μg of biotin-labeled LPS, 10 μg of biotin-labeled LPS plus 20 μg of LPS, or 10 μg of LPS alone. Following incubation, biotin-LPS was pulled down by streptavidin-Sepharose. Captured complexes were washed, and proteins were eluted from the Sepharose and probed for Lrch4 and CD14, in parallel with probing of whole cell lysate.

Statistical analysis

Analysis was performed using GraphPad Prism software (San Diego, CA). The data are represented as means ± S.E. Two-tailed Student's t test was applied for comparisons of two groups, and analysis of variance for comparisons of >2 groups. For all tests, $p < 0.05$ was considered significant.

Author contributions—J. J. A., J. J. G., J. H. M., K. A. G., G. A. M., A. G., B. A. M., and M. B. F. conceptualization; J. J. A., K. M. A., J. J. G., K. M. G., J. H. M., K. A. G., G. A. M., W.-C. L., J. M. L., A. G., M. W. H., D. W. D., B. A. M., and M. B. F. formal analysis; J. J. A., K. M. A., J. J. G., K. M. G., J. H. M., K. A. G., G. A. M., W.-C. L., J. M. L., A. G., M. W. H., D. W. D., B. A. M., and M. B. F. investigation; J. J. A., K. M. A., J. J. G., K. M. G., G. A. M., and A. G. methodology; J. J. A., A. G., and M. B. F. writing-original draft; J. J. A., K. M. A., J. J. G., K. M. G., J. H. M., K. A. G., G. A. M., W.-C. L., J. M. L., A. G., M. W. H., D. W. D., B. A. M., and M. B. F. writing-review and editing; M. B. F. supervision; M. B. F. funding acquisition.

Acknowledgments—We acknowledge the NIEHS Viral Vector Core Facility, the NIEHS Fluorescence Microscopy & Imaging Center, and the NIEHS Flow Cytometry Core Facility.

References

1. Kawai, T., and Akira, S. (2011) Toll-like receptors and their crosstalk with other innate receptors in infection and immunity. *Immunity* **34,** 637–650 CrossRef Medline
2. Kawai, T., and Akira, S. (2010) The role of pattern-recognition receptors in innate immunity: update on Toll-like receptors. *Nat. Immunol.* **11,** 373–384 CrossRef Medline
3. Pasare, C., and Medzhitov, R. (2004) Toll-like receptors and acquired immunity. *Semin. Immunol.* **16,** 23–26 CrossRef Medline
4. Hennessy, E. J., Parker, A. E., and O'Neill, L. A. (2010) Targeting Toll-like receptors: emerging therapeutics? *Nat. Rev. Drug Discov.* **9,** 293–307 CrossRef Medline
5. Lee, C. C., Avalos, A. M., and Ploegh, H. L. (2012) Accessory molecules for Toll-like receptors and their function. *Nat. Rev. Immunol.* **12,** 168–179 CrossRef Medline
6. Park, B. S., Song, D. H., Kim, H. M., Choi, B. S., Lee, H., and Lee, J. O. (2009) The structural basis of lipopolysaccharide recognition by the TLR4-MD-2 complex. *Nature* **458,** 1191–1195 CrossRef Medline
7. Blumenthal, A., Kobayashi, T., Pierini, L. M., Banaei, N., Ernst, J. D., Miyake, K., and Ehrt, S. (2009) RP105 facilitates macrophage activation by *Mycobacterium tuberculosis* lipoproteins. *Cell Host Microbe* **5,** 35–46 CrossRef Medline
8. Divanovic, S., Trompette, A., Atabani, S. F., Madan, R., Golenbock, D. T., Visintin, A., Finberg, R. W., Tarakhovsky, A., Vogel, S. N., Belkaid, Y., Kurt-Jones, E. A., and Karp, C. L. (2005) Negative regulation of Toll-like receptor 4 signaling by the Toll-like receptor homolog RP105. *Nat. Immunol.* **6,** 571–578 CrossRef Medline
9. Carpenter, S., Carlson, T., Dellacasagrande, J., Garcia, A., Gibbons, S., Hertzog, P., Lyons, A., Lin, L. L., Lynch, M., Monie, T., Murphy, C., Seidl, K. J., Wells, C., Dunne, A., and O'Neill, L. A. (2009) TRIL, a functional component of the TLR4 signaling complex, highly expressed in brain. *J. Immunol.* **183,** 3989–3995 CrossRef Medline
10. Yang, Y., Liu, B., Dai, J., Srivastava, P. K., Zammit, D. J., Lefrançois, L., and Li, Z. (2007) Heat shock protein gp96 is a master chaperone for toll-like receptors and is important in the innate function of macrophages. *Immunity* **26,** 215–226 CrossRef Medline
11. Takahashi, K., Shibata, T., Akashi-Takamura, S., Kiyokawa, T., Wakabayashi, Y., Tanimura, N., Kobayashi, T., Matsumoto, F., Fukui, R., Kouro, T., Nagai, Y., Takatsu, K., Saitoh, S., and Miyake, K. (2007) A protein associated with Toll-like receptor (TLR) 4 (PRAT4A) is required for TLR-dependent immune responses. *J. Exp. Med.* **204,** 2963–2976 CrossRef Medline
12. Tabeta, K., Hoebe, K., Janssen, E. M., Du, X., Georgel, P., Crozat, K., Mudd, S., Mann, N., Sovath, S., Goode, J., Shamel, L., Herskovits, A. A., Portnoy, D. A., Cooke, M., Tarantino, L. M., *et al.* (2006) The Unc93b1 mutation 3d disrupts exogenous antigen presentation and signaling via Toll-like receptors 3, 7 and 9. *Nat. Immunol.* **7,** 156–164 CrossRef Medline
13. Dhungana, S., Merrick, B. A., Tomer, K. B., and Fessler, M. B. (2009) Quantitative proteomics analysis of macrophage rafts reveals compartmentalized activation of the proteasome and of proteasome-mediated ERK activation in response to lipopolysaccharide. *Mol. Cell. Proteomics* **8,** 201–213 CrossRef Medline
14. Larkin, M. A., Blackshields, G., Brown, N. P., Chenna, R., McGettigan, P. A., McWilliam, H., Valentin, F., Wallace, I. M., Wilm, A., Lopez, R., Thompson, J. D., Gibson, T. J., and Higgins, D. G. (2007) Clustal W and Clustal X version 2.0. *Bioinformatics* **23,** 2947–2948 CrossRef Medline
15. Hofmann, K. (1993) TMBASE: a database of membrane spanning protein segments. *Biol. Chem. Hoppe-Seyler* **374,** 166
16. Reynolds, S. M., Käll, L., Riffle, M. E., Bilmes, J. A., and Noble, W. S. (2008) Transmembrane topology and signal peptide prediction using dynamic bayesian networks. *PLoS Comput. Biol.* **4,** e1000213 CrossRef Medline
17. Dolan, J., Walshe, K., Alsbury, S., Hokamp, K., O'Keeffe, S., Okafuji, T., Miller, S. F., Tear, G., and Mitchell, K. J. (2007) The extracellular leucine-rich repeat superfamily; a comparative survey and analysis of evolutionary relationships and expression patterns. *BMC Genomics* **8,** 320 CrossRef Medline

18. Ng, A. C., Eisenberg, J. M., Heath, R. J., Huett, A., Robinson, C. M., Nau, G. J., and Xavier, R. J. (2011) Human leucine-rich repeat proteins: a genome-wide bioinformatic categorization and functional analysis in innate immunity. *Proc. Natl. Acad. Sci. U.S.A.* **108,** (Suppl. 1) 4631–4638
19. Lobley, A., Sadowski, M. I., and Jones, D. T. (2009) pGenTHREADER and pDomTHREADER: new methods for improved protein fold recognition and superfamily discrimination. *Bioinformatics* **25,** 1761–1767 CrossRef Medline
20. Sjöblom, B., Ylänne, J., and Djinovic-Carugo, K. (2008) Novel structural insights into F-actin-binding and novel functions of calponin homology domains. *Curr. Opin. Struct. Biol.* **18,** 702–708 CrossRef Medline
21. Foussard, H., Ferrer, P., Valenti, P., Polesello, C., Carreno, S., and Payre, F. (2010) LRCH proteins: a novel family of cytoskeletal regulators. *PLoS One* **5,** e12257 CrossRef Medline
22. Gokhale, N. A., Zaremba, A., Janoshazi, A. K., Weaver, J. D., and Shears, S. B. (2013) PPIP5K1 modulates ligand competition between diphosphoinositol polyphosphates and PtdIns(3,4,5)P3 for polyphosphoinositide-binding domains. *Biochem. J.* **453,** 413–426 CrossRef Medline
23. Alper, S., Laws, R., Lackford, B., Boyd, W. A., Dunlap, P., Freedman, J. H., and Schwartz, D. A. (2008) Identification of innate immunity genes and pathways using a comparative genomics approach. *Proc. Natl. Acad. Sci. U.S.A.* **105,** 7016–7021 CrossRef Medline
24. Trompette, A., Divanovic, S., Visintin, A., Blanchard, C., Hegde, R. S., Madan, R., Thorne, P. S., Wills-Karp, M., Gioannini, T. L., Weiss, J. P., and Karp, C. L. (2009) Allergenicity resulting from functional mimicry of a Toll-like receptor complex protein. *Nature* **457,** 585–588 CrossRef Medline
25. Björkbacka, H., Fitzgerald, K. A., Huet, F., Li, X., Gregory, J. A., Lee, M. A., Ordija, C. M., Dowley, N. E., Golenbock, D. T., and Freeman, M. W. (2004) The induction of macrophage gene expression by LPS predominantly utilizes Myd88-independent signaling cascades. *Physiol. Genomics* **19,** 319–330 CrossRef Medline
26. O'Neill, L. A., and Bowie, A. G. (2007) The family of five: TIR-domain-containing adaptors in Toll-like receptor signalling. *Nat. Rev. Immunol.* **7,** 353–364 CrossRef Medline
27. Yvan-Charvet, L., Welch, C., Pagler, T. A., Ranalletta, M., Lamkanfi, M., Han, S., Ishibashi, M., Li, R., Wang, N., and Tall, A. R. (2008) Increased inflammatory gene expression in ABC transporter-deficient macrophages: free cholesterol accumulation, increased signaling via toll-like receptors, and neutrophil infiltration of atherosclerotic lesions. *Circulation* **118,** 1837–1847 CrossRef Medline
28. Gale, S. C., Gao, L., Mikacenic, C., Coyle, S. M., Rafaels, N., Murray Dudenkov, T., Madenspacher, J. H., Draper, D. W., Ge, W., Aloor, J. J., Azzam, K. M., Lai, L., Blackshear, P. J., Calvano, S. E., Barnes, K. C., *et al.* (2014) APOε4 is associated with enhanced *in vivo* innate immune responses in human subjects. *J. Allergy Clin. Immunol.* **134,** 127–134 CrossRef Medline
29. Triantafilou, M., Miyake, K., Golenbock, D. T., and Triantafilou, K. (2002) Mediators of innate immune recognition of bacteria concentrate in lipid rafts and facilitate lipopolysaccharide-induced cell activation. *J. Cell Sci.* **115,** 2603–2611 Medline
30. Fessler, M. B., and Parks, J. S. (2011) Intracellular lipid flux and membrane microdomains as organizing principles in inflammatory cell signaling. *J. Immunol.* **187,** 1529–1535 CrossRef Medline
31. Siner, J. M., Jiang, G., Cohen, Z. I., Shan, P., Zhang, X., Lee, C. G., Elias, J. A., and Lee, P. J. (2007) VEGF-induced heme oxygenase-1 confers cytoprotection from lethal hyperoxia in vivo. *FASEB J.* **21,** 1422–1432 CrossRef Medline
32. Lee, C. C., Huang, H. Y., and Chiang, B. L. (2008) Lentiviral-mediated GATA-3 RNAi decreases allergic airway inflammation and hyperresponsiveness. *Mol. Ther.* **16,** 60–65 CrossRef Medline
33. Madenspacher, J. H., Azzam, K. M., Gowdy, K. M., Malcolm, K. C., Nick, J. A., Dixon, D., Aloor, J. J., Draper, D. W., Guardiola, J. J., Shatz, M., Menendez, D., Lowe, J., Lu, J., Bushel, P., Li, L., *et al.* (2013) p53 Integrates host defense and cell fate during bacterial pneumonia. *J. Exp. Med.* **210,** 891–904 CrossRef Medline
34. Jha, S. S., Danelishvili, L., Wagner, D., Maser, J., Li, Y. J., Moric, I., Vogt, S., Yamazaki, Y., Lai, B., and Bermudez, L. E. (2010) Virulence-related *Mycobacterium avium* subsp. hominissuis MAV_2928 gene is associated with vacuole remodeling in macrophages. *BMC Microbiol.* **10,** 100 CrossRef Medline
35. Ceppi, M., Pereira, P. M., Dunand-Sauthier, I., Barras, E., Reith, W., Santos, M. A., and Pierre, P. (2009) MicroRNA-155 modulates the interleukin-1 signaling pathway in activated human monocyte-derived dendritic cells. *Proc. Natl. Acad. Sci. U.S.A.* **106,** 2735–2740 CrossRef Medline
36. Hong, M. G., Myers, A. J., Magnusson, P. K., and Prince, J. A. (2008) Transcriptome-wide assessment of human brain and lymphocyte senescence. *PLoS One* **3,** e3024 CrossRef Medline
37. Jiang, Z., Georgel, P., Du, X., Shamel, L., Sovath, S., Mudd, S., Huber, M., Kalis, C., Keck, S., Galanos, C., Freudenberg, M., and Beutler, B. (2005) CD14 is required for MyD88-independent LPS signaling. *Nat. Immunol.* **6,** 565–570 CrossRef Medline
38. Di Gioia, M., and Zanoni, I. (2015) Toll-like receptor co-receptors as master regulators of the immune response. *Mol. Immunol.* **63,** 143–152 CrossRef Medline
39. Raby, A. C., Le Bouder, E., Colmont, C., Davies, J., Richards, P., Coles, B., George, C. H., Jones, S. A., Brennan, P., Topley, N., and Labéta, M. O. (2009) Soluble TLR2 reduces inflammation without compromising bacterial clearance by disrupting TLR2 triggering. *J. Immunol.* **183,** 506–517 CrossRef Medline
40. Liu, S., Morris, S. M., Jr., Nie, S., Shapiro, R. A., and Billiar, T. R. (2000) cAMP induces CD14 expression in murine macrophages via increased transcription. *J. Leukocyte Biol.* **67,** 894–901 CrossRef Medline
41. Rahimi, A. A., Gee, K., Mishra, S., Lim, W., and Kumar, A. (2005) STAT-1 mediates the stimulatory effect of IL-10 on CD14 expression in human monocytic cells. *J. Immunol.* **174,** 7823–7832 CrossRef Medline
42. Liu, S., Shapiro, R. A., Nie, S., Zhu, D., Vodovotz, Y., and Billiar, T. R. (2000) Characterization of rat CD14 promoter and its regulation by transcription factors AP1 and Sp family proteins in hepatocytes. *Gene* **250,** 137–147 CrossRef Medline
43. Pan, Z., Hetherington, C. J., and Zhang, D. E. (1999) CCAAT/enhancer-binding protein activates the CD14 promoter and mediates transforming growth factor β signaling in monocyte development. *J. Biol. Chem.* **274,** 23242–23248 CrossRef Medline
44. Murphy, A. J., Akhtari, M., Tolani, S., Pagler, T., Bijl, N., Kuo, C. L., Wang, M., Sanson, M., Abramowicz, S., Welch, C., Bochem, A. E., Kuivenhoven, J. A., Yvan-Charvet, L., and Tall, A. R. (2011) ApoE regulates hematopoietic stem cell proliferation, monocytosis, and monocyte accumulation in atherosclerotic lesions in mice. *J. Clin. Invest.* **121,** 4138–4149 CrossRef Medline
45. Murphy, A. J., Woollard, K. J., Hoang, A., Mukhamedova, N., Stirzaker, R. A., McCormick, S. P., Remaley, A. T., Sviridov, D., and Chin-Dusting, J. (2008) High-density lipoprotein reduces the human monocyte inflammatory response. *Arterioscler. Thromb. Vasc. Biol.* **28,** 2071–2077 CrossRef Medline
46. Zhu, X., Lee, J. Y., Timmins, J. M., Brown, J. M., Boudyguina, E., Mulya, A., Gebre, A. K., Willingham, M. C., Hiltbold, E. M., Mishra, N., Maeda, N., and Parks, J. S. (2008) Increased cellular free cholesterol in macrophage-specific Abca1 knock-out mice enhances pro-inflammatory response of macrophages. *J. Biol. Chem.* **283,** 22930–22941 CrossRef Medline
47. Zhu, X., Owen, J. S., Wilson, M. D., Li, H., Griffiths, G. L., Thomas, M. J., Hiltbold, E. M., Fessler, M. B., and Parks, J. S. (2010) Macrophage ABCA1 reduces MyD88-dependent Toll-like receptor trafficking to lipid rafts by reduction of lipid raft cholesterol. *J. Lipid Res.* **51,** 3196–3206 CrossRef Medline
48. Zhao, F., Zhang, J., Liu, Y. S., Li, L., and He, Y. L. (2011) Research advances on flotillins. *Virol. J.* **8,** 479 CrossRef Medline
49. Chen, G. Y., and Nuñez, G. (2010) Sterile inflammation: sensing and reacting to damage. *Nat. Rev. Immunol.* **10,** 826–837 CrossRef Medline
50. Salmon, P., and Trono, D. (2006) Production and titration of lentiviral vectors. *Curr. Protoc. Neurosci.* **37,** 4.21.1–4.21.24 CrossRef Medline
51. Ran, F. A., Hsu, P. D., Wright, J., Agarwala, V., Scott, D. A., and Zhang, F. (2013) Genome engineering using the CRISPR-Cas9 system. *Nat. Protoc.* **8,** 2281–2308 CrossRef Medline
52. Ward, J. J., McGuffin, L. J., Bryson, K., Buxton, B. F., and Jones, D. T. (2004) The DISOPRED server for the prediction of protein disorder. *Bioinformatics* **20,** 2138–2139 CrossRef Medline